

Study of the Effect of Cu^{2+} in the Lattice Dynamics of Doped Magnetites Obtained by the Hydrothermal Synthesis Method

A. A. Velásquez¹, J. P. Urquijo²

¹Grupo de Electromagnetismo Aplicado, Universidad EAFIT, Medellín, Colombia; ²Grupo de Estado Sólido, Universidad de Antioquia, Medellín, Colombia.

Email: avelas26@eafit.edu.co

Received July 26th, 2013; revised August 28th, 2013; accepted September 7th, 2013

Copyright © 2013 A. A. Velásquez, J. P. Urquijo. This is an open access article distributed under the Creative Commons Attribution License, which permits unrestricted use, distribution, and reproduction in any medium, provided the original work is properly cited.

ABSTRACT

In this work, the effect of Cu^{2+} on the structural and magnetic properties of samples of magnetite is addressed. Samples of magnetite, both pure and Cu^{2+} doped, $\text{Fe}_{3-x}\text{Cu}_x\text{O}_4$, with $x = 0, 5, 10$ and 20 atm.% were synthesized hydrothermally. The two-lattice method was employed to measure the Mössbauer recoilless fraction of magnetite relative to hematite ($f_{\text{mag}}/f_{\text{hem}}$) of the samples, looking for evidence of substitution of Fe^{2+} by Cu^{2+} . The relative recoilless fraction measurements were performed by taking room temperature Mössbauer spectra of mixtures of each sample with analytical grade hematite. The Mössbauer measurements were complemented with Atomic Absorption Spectroscopy (AAS) and Energy Dispersive X-ray Spectroscopy (EDS). The analyses by AAS and EDS showed that the copper concentration in the final products increases with increasing the content of Cu^{2+} in the starting solutions. The Mössbauer analyses showed a linear decrease trend of the relative Mössbauer recoilless fraction with increasing concentration of Cu^{2+} in the samples, as well as a reduction in the hyperfine magnetic field, which was more significant in the octahedral sites than tetrahedral sites. The broadening of the Mössbauer spectral lines was more significant for the octahedral sub spectrum than for the tetrahedral sub spectrum. Our study points that Cu^{2+} occupies preferentially the octahedral sites, where it substitutes Fe^{2+} species, generating broadening in the lines of the octahedral sub spectrum and a reduction in the probability of having nuclear resonant absorption of Mössbauer gamma rays in the samples.

Keywords: Doped Magnetites; Mössbauer Recoilless Fraction; Divalent Copper

1. Introduction

Since its discovery, magnetite has attracted the attention of many investigators given its multiple possibilities of application in several fields, such as information storage media [1,2], magnetic paints, magnetic fluids, pigments, contrast mean for clinical analysis [3,4], corrosion products of steels [5,6], chemical sensors, spintronic devices [7-9], among others. The synthesis of magnetite in presence of divalent and trivalent cations of transition metals such as V^{3+} , Cr^{3+} , Mn^{2+} , Co^{2+} , Ni^{2+} and Cu^{2+} has been very studied in the last decades due to that these cations can modify the magnetic, electrical and structural properties of this iron oxide, which makes it possible to find the proper material for a specific application, or help to understand the mechanism of formation of rusts in alloy steels which contain some of these cations. To mention some of these works, Sidhu, Gilkes and Posner [10]

found that the surface area of magnetite particles synthesized in presence of Cu^{2+} is larger than that of the particles of non doped magnetites. By transmission electron microscopy measurements, they found that the particle size of the magnetites doped with Cu^{2+} is smaller than the particle size of nondoped magnetites. Additional analyses by dissolution of the doped magnetites in HCl solutions showed a tendency of the Cu^{2+} cations to migrate towards the surface of the grains instead of the volume. Ishikawa, Nakazaki, Yasukawa, Kandori and Seto [11,12] investigated the influence of cations such as Cu^{2+} , Ti^{4+} , Ni^{2+} and Cr^{3+} in the formation of several iron oxides, especially magnetite. They found that only a fraction of Cu^{2+} present in the starting solution was incorporated within the structure of the magnetite and that the particle size decreases as the content of this cation increases. The crystallite size decreased from 47 nm to 20 nm as the

copper content increased. The authors argue that it is not possible to know where copper cations are incorporated in the structure. Sorescu, Oberst, Gosset, Tarabasanu and Diamandescu [13-15] synthesized hydrothermally samples of magnetite doped with Co^{2+} in percentages from 0 to 60 atm.% and characterized the samples by room temperature Mössbauer spectroscopy. Their results showed that Co^{2+} is incorporated preferentially in the octahedral sites, because the magnetic hyperfine field increased appreciably in these sites while remained almost constant in the tetrahedral sites, and the area of the octahedral sub spectrum decreased. They also suggest that Co^{2+} introduces disorder in the structure of the magnetite because the Mössbauer spectral lines are broad. Kim and Lee [16] studied comparatively magnetite and copper-ferrite, both in cubic phase. In the copper-ferrite it was found that Cu^{2+} occupies entirely the octahedral sites, substituting Fe^{2+} , this sample also showed tetragonal Jahn-Teller distortion, where a copper ion centred in an octahedron interacts strongly with oxygen atoms placed in the octahedron plane, but weakly with the oxygen atoms perpendicular to this plane. As a consequence, the octahedron is distorted, elongating in the direction of weaker interaction.

In a previous investigation [17], we employed the hydrothermal method to synthesize samples of magnetite, both pure and doped with Cu^{2+} , $\text{Fe}_{3-x}\text{Cu}_x\text{O}_4$, with $x = 0, 5, 10$ and 20 atm.%, which were characterized by chemical, structural and magnetic analysis techniques, such as Atomic Absorption Spectroscopy, X-ray diffraction, room temperature Mössbauer Spectroscopy and SQUID magnetometry. Changes in the structural and magnetic properties of the samples were observed with the addition of Cu^{2+} to the starting solutions. The mean crystallite size, particle size and lattice parameter of the samples diminished sequentially with increasing amount of Cu^{2+} , the morphology of the particles changed from cubical for the nondoped sample to undefined for the sample with $x = 20$ atm.%. The hyperfine magnetic field showed more reduction at octahedral sites than tetrahedral sites and the saturation magnetization was reduced from 77.5 emu/g for the non doped sample to 67.1 emu/g for the sample with $x = 20$ atm.%. These analyses suggested one or two combined effects of Cu^{2+} in the structure of the magnetite, the first effect is its incorporation in the structure, preferentially in the octahedral sites, replacing Fe^{2+} species, and the second one is the promotion of vacancies at octahedral sites.

Looking for additional evidence of the effects of Cu^{2+} on the structural properties of magnetite, we report the results derived from a subsequent investigation performed on this same set of samples, in which we studied the effects caused by Cu^{2+} in the lattice dynamics of the samples through measurements of Mössbauer recoilless

fraction of the magnetite relative to analytical hematite, because the Mössbauer recoilless fraction, also termed f factor, is very sensitive to changes in the lattice dynamics caused by different reasons, among them substitution of Mössbauer nuclei in crystalline sites. The experimental details and the conclusions obtained from these measurements are presented through this paper.

2. Experimental Procedure

2.1. Preparation of the Samples

The magnetites were obtained by the hydrothermal synthesis method reported by Cornell and Schwertmann [18]. We used $\text{FeCl}_2 \cdot 4\text{H}_2\text{O}$ as Fe^{2+} precursor and NaNO_3 as Fe^{2+} oxidant. For the synthesis of nondoped magnetite we start from 0.1 M (300 ml) $\text{FeCl}_2 \cdot 4\text{H}_2\text{O}$ aqueous solution, which was constantly bubbled with $\text{N}_{2(g)}$ and heated in a thermal bath at 90°C . When the thermal equilibrium was reached, 100 ml of alkaline mixture composed of NaOH 3 M and NaNO_3 0.06 M were added dropwise to the before solution during a time of 5 min. Finished the addition of the alkaline mixture, the reaction continued at 90°C during 30 min, with permanent stirring at 300 rpm and deaeration with $\text{N}_{2(g)}$. When the reaction finished, the black precipitate was washed repeatedly with deionized water to obtain a neutral pH in the residual supernatant. To remove water molecules of the precipitate this was filtered and dried in an oven at 40°C for 48 h, after which powdered magnetite was obtained. For an efficient washing and drying of the reaction product, this was divided in two parts, the first part was taken from the precipitate accumulated on the bottom of the reaction vessel, while the second part, which was used for this investigation, was the remainder precipitate taken from the reaction vessel.

The magnetites doped with Cu^{2+} were prepared from 300 ml of aqueous solutions 0.1 M in $\text{FeCl}_2 \cdot 4\text{H}_2\text{O}$ and 1.662×10^{-3} M, 3.324×10^{-3} M and 6.648×10^{-3} M in $\text{CuCl}_2 \cdot 2\text{H}_2\text{O}$ for $5, 10$ and 20 atm.%- Cu^{2+} , respectively. The subsequent procedure was the same described for the nondoped magnetite. According to the doping percentage, the samples were labeled: mag0cu, mag5cu, mag10cu and mag20cu for $x = 0, 5, 10$ and 20 atm.%- Cu^{2+} respectively.

2.2. Experimental Techniques

Atomic Absorption Spectroscopy (AAS) measurements were performed with an UNICAM 929 AA spectrometer with copper lamp. The samples were first diluted in HCl solutions for these measurements. Energy Dispersive X-ray Spectroscopy (EDS) spectra were taken with a Low Vacuum Scanning Electron Microscopy JEOL model JSM-6460LV, operating at voltages of 20 kV. Room temperature Mössbauer spectra were taken with a spec-

trometer developed in our laboratory, which operates with a ⁵⁷Co/Rh radioactive source, 512 channels and a triangular velocity waveform, thin absorbers with disk shape and effective thickness of 6 mg/cm² of iron were prepared for these measurements.

3. Results and Discussion

3.1. Atomic Absorption Analyses

To quantify the concentration of copper present in the doped samples, we made atomic absorption measurements, the results are presented in **Table 1**, which shows the weight percentages of copper measured in the doped samples, the expected copper concentrations calculated from the initial solutions prepared and the substitution parameter x calculated from these results. These same results were reported in [17] because the samples were obtained from the same reaction product in all cases. From **Table 1**, it can be observed that the copper concentration measured in the samples increases as the copper content increases in the synthesis process, being the weight percentage of copper close to 70% of the initial copper present in the synthesis of each doped sample.

3.2. EDS Analyses

The EDS spectra of the samples are presented in **Figure 1**. These spectra show an increase of the intensity of the copper peaks as the Cu²⁺ content increases in the synthesis process, which is an indication that increasing amount of Cu²⁺ is being incorporated within the structure of the doped samples as the concentration of Cu²⁺ increases in the starting solutions. Although EDS measurements have a more qualitative than quantitative character in this work, it is important to notice that the increasing content of the copper concentration obtained by EDS from an arbitrary region of the samples with a volume of the order of 1 μm³ is consistent with the information obtained by Atomic Absorption Spectroscopy for the bulk samples, which suggests a homogeneous distribution of the copper in the samples.

Table 1. Weight percentage of copper found in the samples by atomic absorption spectroscopy.

| Sample | Measured copper concentration (%wt) | Expected copper concentration (%wt) | Substitution parameter calculated x |
|---------|-------------------------------------|-------------------------------------|---------------------------------------|
| mag0cu | Nondoped | Nondoped | 0 |
| mag5cu | 1.14 ± 0.02 | 1.62 | 0.035 |
| mag10cu | 2.32 ± 0.04 | 3.24 | 0.072 |
| mag20cu | 4.78 ± 0.09 | 6.48 | 0.148 |

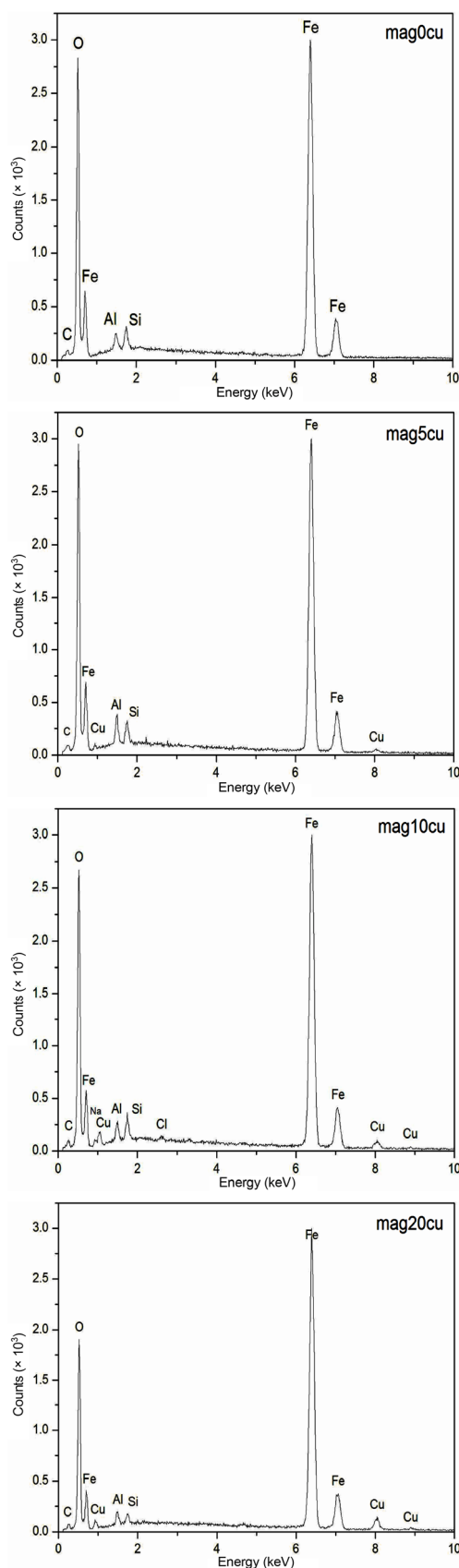


Figure 1. EDS spectra of the samples.

3.3. Estimation of the Relative Mössbauer Recoilless Fraction (f_{mag}/f_{hem})

The Mössbauer recoilless fraction, also termed f factor, measures the probability of having absorption or emission of Mössbauer gamma rays without energy loss by recoil of the Mössbauer nuclei [19]. Several parameters can affect its magnitude among them are the Debye temperature of the solid, the external temperature applied to the sample, crystalline defects, particle size [20] and substituent elements in the structure of the solid, which replace resonant Mössbauer nuclei. Substituent cations can reduce the bonding strength between the resonant nuclei and their ligands, reducing the probability of having a zero phonon process. A good experiment to measure the Mössbauer recoilless fraction is the two-lattice absorber method, reported by Sorescu [20]. According to this method, if a powder sample under study is mixed with a reference powder phase, whose Mössbauer recoilless fraction is known, then the unknown Mössbauer recoilless fraction of the sample can be estimated from a room temperature Mössbauer spectrum according to the relation:

$$\frac{f_s}{f_r} = \frac{N_r(^{57}\text{Fe})A_s}{N_s(^{57}\text{Fe})A_r} = \frac{aN_r(\text{Fe})A_s}{aN_s(\text{Fe})A_r} = \frac{N_r(\text{Fe})A_s}{N_s(\text{Fe})A_r} \quad (1)$$

where:

f_s, f_r : Mössbauer recoilless fraction of the sample and reference phase;

a : isotopic abundance of the ⁵⁷Fe ≈ 2.2%;

$N_s(^{57}\text{Fe}), N_r(^{57}\text{Fe})$: number of Mössbauer nuclei in the sample and reference phase;

$N_s(\text{Fe}), N_r(\text{Fe})$: number of Fe atoms in the sample and reference phase;

A_s, A_r : Mössbauer spectral areas of the sample and reference phase.

By applying chemical arguments, the number of iron atoms in each phase can be expressed in terms of the mass and molecular weight of the phase according to the relation:

$$\frac{f_s}{f_r} = \frac{g_r y_r W_s A_s}{g_s y_s W_r A_r} \quad (2)$$

where:

g_s, g_r : mass of the sample and reference phase;

y_s, y_r : number of iron atoms per chemical formula in the sample and reference phase;

W_s, W_r : molar weight of the sample and reference phase.

In our experiment each sample was mixed with the same quantity of analytical grade hematite (Analysis Oxide α -Fe₂O₃, Merck KgaA), the masses of both phases were calculated to obtain approximately the same con-

tribution of iron atoms per phase to the mixture. The values of the parameters g, y and W , described before, are presented in **Table 2**.

By replacing the parameters given in **Table 2** in the Equation (2), the ratio between the Mössbauer recoilless fractions of magnetite and hematite can be expressed in terms of their relative areas in the Mössbauer spectrum of the mixture, as follows:

$$\frac{f_{mag}}{f_{hem}} = \frac{2.9}{3-x} \frac{A_{mag}}{A_{hem}} \quad (3)$$

As the hematite used in all mixtures was the same, its Mössbauer recoilless fraction can be assumed constant, in this way, the changes observed in the ratio f_{mag}/f_{hem} can be attributed only to the changes in the magnitude f_{mag} .

Room temperature Mössbauer spectra of the mixtures are shown in **Figure 2**, the hyperfine parameters of the spectra obtained by least squares fitting with the program MOSF [21] and the spectral areas are presented in **Tables 3** and **4**. All spectra were fitted with one sextet for hematite, one sextet for tetrahedral sites of magnetite, one sextet for octahedral sites of magnetite and a doublet attributed to superparamagnetic goethite (α -FeOOH), whose spectral area was lower than 2% in all spectra. The percentage of goethite was too small to be taken into account in our calculations. Goethite may form in the hydrothermal synthesis of iron oxides due to easy formation of iron hydroxides under the conditions here present [18]. It is important to note here that all Mössbauer spectra of the samples studied in [17] were fitted with a small sextet of magnetic goethite, whose spectral area varied between 4% and 8%. This magnetic phase was not identified in the spectra of the mixtures. We attribute this fact to a lower particle size of the goethite present in the last precipitate recovered from the reaction vessel, which contains particles whose precipitation rate is slowed by their smaller particle size, which could explain that only superparamagnetic goethite was observed in all samples.

The **Table 3** shows that the hyperfine magnetic field decreases more in the octahedral sites than in the tetrahedral sites, the linewidth of the octahedral sub spectrum increases while the linewidth of the tetrahedral sub spectrum remains nearly constant within the error bar of this parameter.

These observations suggest that the dominant effect of the Cu²⁺ in the synthesis process is its incorporation in

Table 2. Parameters of the Equation (2) for magnetite and hematite.

| Phase | g (mg) | y | W (g/mol) |
|-----------|----------|-------|-------------|
| Magnetite | 10 | $3-x$ | 231.5 |
| Hematite | 10 | 2 | 159.7 |

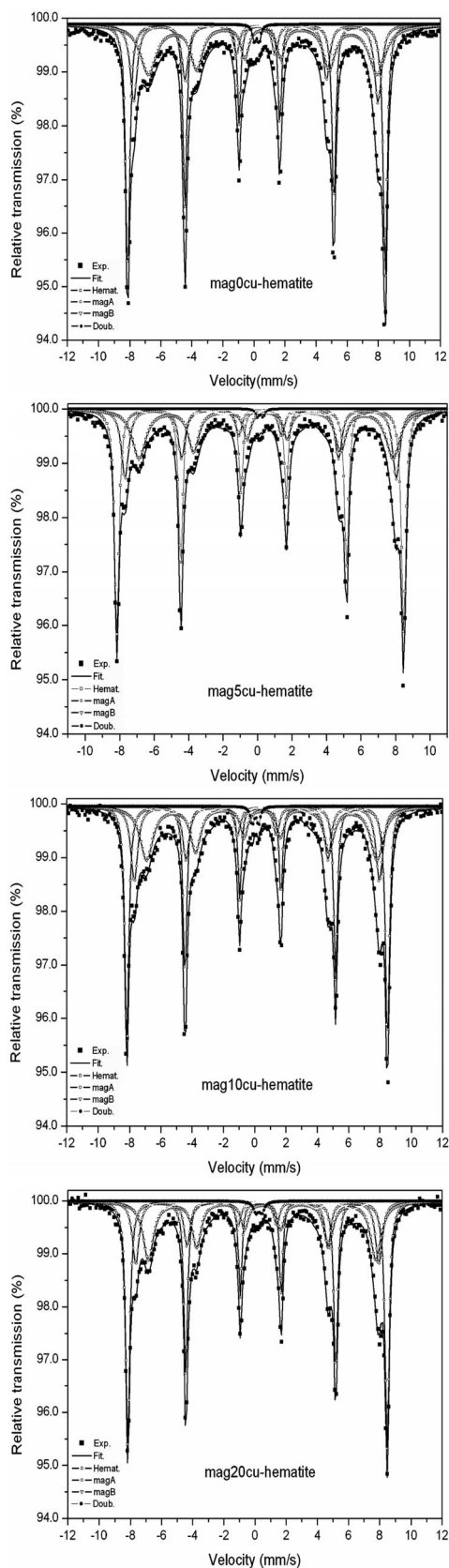


Figure 2. Room temperature Mössbauer spectra of the mixtures magnetite-hematite.

Table 3. Mössbauer parameters of the samples.

| Sample | $B_{\text{hf-hem}} (\pm 0.2 \text{ T})$ | $B_{\text{hf-magA}} (\pm 0.2 \text{ T})$ | $B_{\text{hf-magB}} (\pm 0.2 \text{ T})$ |
|------------------|---|--|--|
| mag0cu-hematite | 51.6 | 48.8 | 45.9 |
| mag5cu-hematite | 51.6 | 48.8 | 45.7 |
| mag10cu-hematite | 51.6 | 48.6 | 45.6 |
| mag20cu-hematite | 51.6 | 48.4 | 45.3 |

| Sample | $IS_{\text{hem}} (\pm 0.02 \text{ mm/s})$ | $IS_{\text{magA}} (\pm 0.02 \text{ mm/s})$ | $IS_{\text{magB}} (\pm 0.02 \text{ mm/s})$ |
|------------------|---|--|--|
| mag0cu-hematite | 0.36 | 0.37 | 0.69 |
| mag5cu-hematite | 0.36 | 0.38 | 0.63 |
| mag10cu-hematite | 0.36 | 0.36 | 0.69 |
| mag20cu-hematite | 0.36 | 0.37 | 0.69 |

| Sample | $QS_{\text{hem}} (\pm 0.02 \text{ mm/s})$ | $QS_{\text{magA}} (\pm 0.02 \text{ mm/s})$ | $QS_{\text{magB}} (\pm 0.02 \text{ mm/s})$ |
|------------------|---|--|--|
| mag0cu-hematite | -0.20 | -0.02 | -0.04 |
| mag5cu-hematite | -0.21 | 0.02 | -0.07 |
| mag10cu-hematite | -0.21 | -0.01 | -0.04 |
| mag20cu-hematite | -0.22 | -0.01 | -0.03 |

| Sample | $W_{\text{hem}} (\pm 0.02 \text{ mm/s})$ | $W_{\text{magA}} (\pm 0.02 \text{ mm/s})$ | $W_{\text{magB}} (\pm 0.02 \text{ mm/s})$ |
|------------------|--|---|---|
| mag0cu-hematite | 0.27 | 0.48 | 0.51 |
| mag5cu-hematite | 0.26 | 0.46 | 0.54 |
| mag10cu-hematite | 0.26 | 0.46 | 0.58 |
| mag20cu-hematite | 0.26 | 0.44 | 0.62 |

| Sample | $A_{\text{hem}} (\%)$ | $A_{\text{mag}} (\%)$ |
|------------------|-----------------------|-----------------------|
| mag0cu-hematite | 43.0 ± 0.8 | 55 ± 1 |
| mag5cu-hematite | 44.4 ± 0.9 | 54 ± 1 |
| mag10cu-hematite | 46.4 ± 0.9 | 52 ± 1 |
| mag20cu-hematite | 49.0 ± 0.9 | 49.6 ± 0.9 |

a. Subscripts hem, magA and magB represent hematite, tetrahedral and octahedral sites of magnetite, respectively, B_{hf} : hyperfine magnetic field, IS: isomer shift relative to $\alpha\text{-Fe}$, QS: quadrupole splitting, W: linewidth of the inner lines and A: spectral area.

the octahedral sites of magnetite, replacing Fe^{2+} cations, and consequently reducing the magnetic interactions in those sites and creating broad and asymmetric lines in the octahedral sub spectrum. These effects are similar to that found in the samples studied in [17], where the reduction in the hyperfine magnetic field and the broadening of the octahedral sub spectrum confirms the distribution of hyperfine magnetic fields produced by the incorporation of

Table 4. Mössbauer parameters of the doublet attributed to superparamagnetic goethite impurity found in all samples.

| Sample | IS ^b (±0.02 mm/s) | QS (±0.02 mm/s) | W (±0.02 mm/s) | A (%) |
|------------------|------------------------------|-----------------|----------------|-------------|
| mag0cu-hematite | 0.16 | 0.31 | 0.27 | 2.00 ± 0.05 |
| mag5cu-hematite | 0.23 | 0.32 | 0.26 | 1.91 ± 0.04 |
| mag10cu-hematite | 0.15 | 0.40 | 0.40 | 1.60 ± 0.03 |
| mag20cu-hematite | 0.36 | 0.38 | 0.40 | 1.40 ± 0.03 |

b. Isomer shifts are relative to α -Fe.

Cu²⁺ in the octahedral sites.

The **Table 5** shows the values of the ratio f_{mag}/f_{hem} obtained by substitution of the spectral areas and the parameter x calculated from atomic absorption measurements in the Equation (3). The **Figure 3** shows the progressive and nearly linear decrease in the ratio f_{mag}/f_{hem} with increasing the content of Cu²⁺ in the precursor solution, which as explained above, is due to a reduction in f_{mag} .

It is well known [22] that when certain cations, among them Cu²⁺, occupy octahedral sites, they tend to distort the crystalline structure through the Jahn-Teller effect, in order to minimize the crystal field stabilization energy.

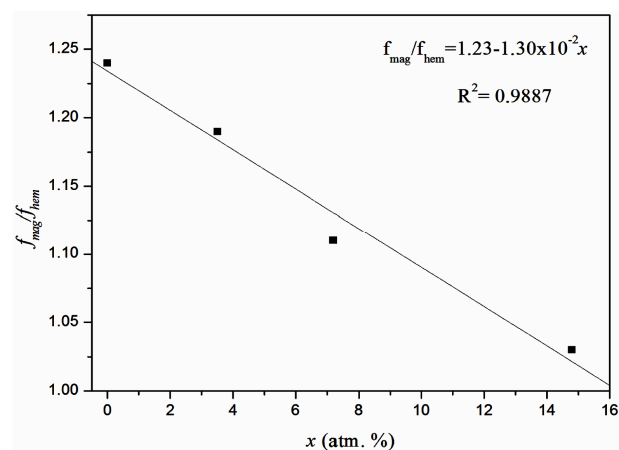
When Cu²⁺ occupies an octahedral site in the structure of the magnetite, the Jahn-Teller distortion produces a weakening of the bonding Cu-O along the direction perpendicular to the octahedron middle plane, this weakening of the bonding Cu-O can rearrange the crystalline structure, reducing the energy necessary to create phonons in the crystalline lattice, which can contribute to the reduction observed in the recoilless Mössbauer fraction of the doped samples.

4. Conclusion

Magnetite samples, both pure and doped with Cu²⁺, were synthesized by the hydrothermal method. Analyses by AAS and EDS showed that globally and locally the copper content in the samples increases successively with the increasing of Cu²⁺ in the synthesis process, being the percentage of copper in the doped samples close to 70% of the copper used in the starting solutions. The presence of Cu²⁺ in the synthesis of magnetite reduces the Mössbauer recoilless fraction of the doped samples, being this reduction nearly linear for the range of doping studied. While the hyperfine parameters derived from the Mössbauer spectra of the mixtures gave similar information for the phase of magnetite than that obtained from non-mixed magnetites studied in [17], the reduction observed in the Mössbauer recoilless fraction of magnetite reinforce our previous hypothesis that the dominant effect of Cu²⁺ in the synthesis process is its incorporation in the octahedral sites of magnetite, where it substitutes Fe²⁺

Table 5. Relative Mössbauer recoilless fraction of the samples.

| Sample | f_{mag}/f_{hem} |
|------------------|-------------------|
| mag0cu-hematite | 1.24 ± 0.04 |
| mag5cu-hematite | 1.19 ± 0.03 |
| mag10cu-hematite | 1.11 ± 0.03 |
| mag20cu-hematite | 1.03 ± 0.03 |

**Figure 3. Variation of the ratio f_{mag}/f_{hem} in function of the atomic Cu²⁺ substitution.**

species and produces Jahn-Teller distortion. Both effects reduce the probability of having resonant absorption of 14.4 keV gamma rays, because substitution reduces the amount of resonant nuclei in the sample while the Jahn-Teller distortion weakens the bonding Cu-O in the structure, reducing the energy necessary to excite phonons in the crystalline lattice. This study provides new evidences for previous works, where the role of Cu²⁺ in magnetite has not been fully understood. On the other hand, the understanding of the effect of the copper in the magnetic and structural properties of magnetite can be useful to researches who work in the design of products based on substituted magnetites, such as doped magnetite paints, doped magnetite inks, doped nanoparticles, doped magnetite thin films, among others.

REFERENCES

- [1] D. Guin and S. V. Manorama, "Room Temperature Synthesis of Monodispersed Iron Oxide Nanoparticles," *Materials Letters*, Vol. 62, No. 17-18, 2008, pp. 3139-3142. <http://dx.doi.org/10.1016/j.matlet.2008.02.005>
- [2] A. A. Novakova, V. Yu. Lanchinskaya, A. V. Volkov, T. S. Gendler, T. Yu. Kiselya, M. A. Moskvina and S. B. Zezin, "Magnetic Properties of Polymer Nanocomposites Containing Iron Oxide Nanoparticles," *Journal of Magnetism and Magnetic Materials*, Vol. 258-259, 2003, pp. 354-357. [http://dx.doi.org/10.1016/S0304-8853\(02\)01062-4](http://dx.doi.org/10.1016/S0304-8853(02)01062-4)
- [3] C. C. Berry and A. S. G. Curtis, "Functionalisation of Magnetic Nanoparticles for Applications in Biomedicine," *Journal of Physics D: Applied Physics*, Vol. 36, No. 13, 2003, pp. 198-206. <http://dx.doi.org/10.1088/0022-3727/36/13/203>
- [4] P. Tartaj, M. del P. Morales, S. Veintemillas-Verdaguer, T. González-Carreño and C. J. Serna, "The Preparation of Magnetic Nanoparticles for Applications in Biomedicine," *Journal of Physics D: Applied Physics*, Vol. 36, No. 13, 2003, pp. 182-197. <http://dx.doi.org/10.1088/0022-3727/36/13/202>
- [5] K. E. García, A. L. Morales, C. A. Barrero and J. M. Greneche, "New Contributions to the Understanding of Rust Layer Formation in Steels Exposed to a Total Immersion Test," *Corrosion Science*, Vol. 48, No. 9, 2006, pp. 2813-2830. <http://dx.doi.org/10.1016/j.corsci.2005.09.002>
- [6] Y. Y. Chen, H. J. Tzeng, L. I. Wei, L. H. Wang, J. C. Oung and H. C. Shih, "Properties of Low-Alloy Steels Under Atmospheric Conditions," *Corrosion Science*, Vol. 47, No. 4, 2005, pp. 1001-1021. <http://dx.doi.org/10.1016/j.corsci.2004.04.009>
- [7] T. Furubayashi, "Magnetite Films Prepared by Reactive Evaporation," *Journal of Magnetism and Magnetic Materials*, Vol. 272-276, 2004, pp. E781-E783
- [8] G. Zhang, C. Fan, L. Pan, F. Wang, P. Wu, H. Qiu, Y. Gu and Y. Zhang, "Magnetic and Transport Properties of Magnetite Thin Films," *Journal of Magnetism and Magnetic Materials*, Vol. 293, No. 2, 2005, pp. 737-745. <http://dx.doi.org/10.1016/j.jmmm.2004.11.529>
- [9] X. Hu, M. Xu, X. Cui and S. Zhang, "Room-Temperature Magnetoresistance Effects of Ag-Added Fe₃O₄ Films with Single-Domain Grains," *Solid State Communications*, Vol. 142, No. 10, 2007, pp. 595-599. <http://dx.doi.org/10.1016/j.ssc.2007.04.004>
- [10] P. S. Sidhu, R. J. Gilkes and A. M. Posner, "The Synthesis and Some Properties of Co, Ni, Zn, Cu, Mn and Cd Substituted Magnetites," *Journal of Inorganic and Nuclear Chemistry*, Vol. 40, No. 3, 1978, pp. 429-435. [http://dx.doi.org/10.1016/0022-1902\(78\)80418-7](http://dx.doi.org/10.1016/0022-1902(78)80418-7)
- [11] T. Ishikawa, H. Nakazaki, A. Yasukawa, K. Kandori and M. Seto, "Influences of Co²⁺, Cu²⁺ and Cr³⁺ Ions on the Formation of Magnetite," *Corrosion Science*, Vol. 41, No. 8, 1999, pp. 1665-1680. [http://dx.doi.org/10.1016/S0010-938X\(98\)00198-X](http://dx.doi.org/10.1016/S0010-938X(98)00198-X)
- [12] T. Ishikawa, M. Kumagai, A. Yasukawa, K. Kandori, T. Nakayama and F. Yuse, "Influences of Metal Ions on the Formation of γ -FeOOH and Magnetite Rusts," *Corrosion Science*, Vol. 44, No. 5, 2002, pp. 1073-1086. [http://dx.doi.org/10.1016/S0010-938X\(01\)00119-6](http://dx.doi.org/10.1016/S0010-938X(01)00119-6)
- [13] M. Sorescu, T. Oberst, K. Gosset, D. Tarabasanu and L. Diamandescu, "Direct Evidence for Cobalt Substitution Effects in Magnetite," *Solid State Communications*, Vol. 113, No. 10, 2000, pp. 573-575. [http://dx.doi.org/10.1016/S0038-1098\(99\)00540-2](http://dx.doi.org/10.1016/S0038-1098(99)00540-2)
- [14] M. Sorescu, T. Oberst, K. Gosset, D. Tarabasanu and L. Diamandescu, "Population Effects in Cobalt-Substituted Magnetite," *Materials Letters*, Vol. 44, No. 2, 2000, pp. 110-112. [http://dx.doi.org/10.1016/S0167-577X\(00\)00012-4](http://dx.doi.org/10.1016/S0167-577X(00)00012-4)
- [15] M. Sorescu, "Recoilless Fraction of Cobalt-Doped Magnetite," *Nuclear Instruments and Methods in Physics Research Section B*, Vol. 269, No. 6, 2011, pp. 590-596. <http://dx.doi.org/10.1016/j.nimb.2011.01.013>
- [16] K. J. Kim, J. H. Lee and S. H. Lee, "Magneto-Optical Investigation of Spinel Ferrite CuFe₂O₄: Observation of Jahn-Teller Effect in Cu_{2p} Ion," *Journal of Magnetism and Magnetic Materials*, Vol. 279, No. 2-3, 2004, pp. 173-177. <http://dx.doi.org/10.1016/j.jmmm.2004.01.078>
- [17] A. L. Morales, A. A. Velásquez, J. P. Urquijo and E. Baggio, "Synthesis and Characterization of Cu²⁺ Substituted Magnetite," *Hyperfine Interactions*, Vol. 203, No. 1-3, 2011, pp. 75-84. <http://dx.doi.org/10.1007/s10751-011-0349-x>
- [18] R. M. Cornell and U. Schwertmann, "The Iron Oxides," Wiley-VCH, Weinheim, 1996.
- [19] L. May, "An Introduction to Mössbauer Spectroscopy," Plenum Press, New York, 1971. <http://dx.doi.org/10.1007/978-1-4684-8911-8>
- [20] M. Sorescu, "Determination of the Recoilless Fraction in Iron Oxide Nanoparticles Using the Two-Lattice Method," *Journal of Nanoparticle Research*, Vol. 4, No. 3, 2002, pp. 221-224. <http://dx.doi.org/10.1023/A:1019960113846>
- [21] R. Vandenberghe, E. de Grave and P. M. A. de Bakker, "On the Methodology of the Analysis of Mössbauer Spectra," *Hyperfine Interactions*, Vol. 83, No. 1, 1994, pp. 29-49. <http://dx.doi.org/10.1007/BF02074257>
- [22] I. Nedkov, R. E. Vandenberghe, T. Marinova, P. Thailhades, T. Merodiiska and I. Avramova, "Magnetic Structure and Collective Jahn-Teller Distortions in Nanostructured Particles of CuFe₂O₄," *Applied Surface Science*, Vol. 253, No. 5, 2006, pp. 2589-2596. <http://dx.doi.org/10.1016/j.apsusc.2006.05.049>